J. Cell. Mol. Med. Vol 20, No 9, 2016 pp. 1686-1695

Mitofusin-2 knockdown increases ER–mitochondria contact and decreases amyloid β-peptide production

Nuno Santos Leal [a], Bernadette Schreiner [a], Catarina Moreira Pinho [a], Riccardo Filadi [b], Birgitta Wiehager [a], Helena Karlström [a], Paola Pizzo [b], Maria Ankarcrona [a, *]

[a] *Center for Alzheimer Research, Division of Neurogeriatrics, Department of Neurobiology, Care Sciences and Society, Karolinska Institutet, Stockholm, Sweden*
[b] *Department of Biomedical Sciences, University of Padua, Padua, Italy*

Received: January 25, 2016; Accepted: March 4, 2016

Abstract

Mitochondria are physically and biochemically in contact with other organelles including the endoplasmic reticulum (ER). Such contacts are formed between mitochondria-associated ER membranes (MAM), specialized subregions of ER, and the outer mitochondrial membrane (OMM). We have previously shown increased expression of MAM-associated proteins and enhanced ER to mitochondria Ca^{2+} transfer from ER to mitochondria in Alzheimer's disease (AD) and amyloid β-peptide (Aβ)-related neuronal models. Here, we report that siRNA knockdown of mitofusin-2 (Mfn2), a protein that is involved in the tethering of ER and mitochondria, leads to increased contact between the two organelles. Cells depleted in Mfn2 showed increased Ca^{2+} transfer from ER to mitchondria and longer stretches of ER forming contacts with OMM. Interestingly, increased contact resulted in decreased concentrations of intra- and extracellular $Aβ_{40}$ and $Aβ_{42}$. Analysis of γ-secretase protein expression, maturation and activity revealed that the low Aβ concentrations were a result of impaired γ-secretase complex function. Amyloid-β precursor protein (APP), β-site APP-cleaving enzyme 1 and neprilysin expression as well as neprilysin activity were not affected by Mfn2 siRNA treatment. In summary, our data shows that modulation of ER–mitochondria contact affects γ-secretase activity and Aβ generation. Increased ER–mitochondria contact results in lower γ-secretase activity suggesting a new mechanism by which Aβ generation can be controlled.

Keywords: Alzheimer's disease • Mitofusin-2 • ER–mitochondria contacts • Aβ • γ-secretase

Introduction

Organelles are dynamic and in contact with each other. One example is the endoplasmic reticulum (ER) that is physically and biochemically connected with the outer membrane of mitochondria (OMM). These connections occur at subregions of the ER membrane referred to as mitochondria-associated ER membranes (MAM). Mitochondria-associated ER membranes are specialized cholesterol-rich stretches of ER membranes with similar properties and composition as lipid rafts [1]. The distance between ER and OMM at the contacts is approximately 20–30 nm [2]. Several proteins have been described to tether ER and mitochondria in mammalian cells. Such proteins include: mitofusin-2 (Mfn2), phosphofurin acidic cluster sorting protein-2, inositol 1,4,5-triphosphate receptor 3 (IP3R3), glucose-regulated protein and voltage-dependent anion channel 1 (VDAC1) [3–6]. Mitofusin-2 is located both in MAM and OMM, while Mfn1 is restricted to the OMM [6]. Previous studies have suggested that mitofusin homo- and heterodimers (Mfn2–Mfn2 and Mfn2–Mfn1) form an ER–mitochondria tethering complex. However, recent data propose that Mfn2 instead acts as a negative regulator, preventing excess of contacts between the two organelles [7–9]. These studies show that reduction of Mfn2 in mouse embryonic fibroblasts results in increased ER–mitochondria coupling and Ca^{2+} transfer [7, 8]. Ca^{2+} is released at MAM *via* the IP3Rs and taken up by mitochondria *via* VDAC1 (in the OMM) and the mitochondrial Ca^{2+} uniporter (MCU, in the inner mitochondrial membrane) [3, 10–12]. Moreover, it has been shown that ER–mitochondria tethering and the Ca^{2+} transfer between the two organelles are enhanced in cells expressing a familial Alzheimer's disease mutation in presenilin-2 (PS2) [13] .

Other functions of MAM and ER–mitochondria communication include: phospholipid and cholesterol synthesis and trafficking, formation of autophagosomal membranes and regulation of apoptosis [14–16]. Interestingly, all these processes are affected in Alzheimer's disease (AD) pathogenesis [1, 10, 17–23]. We have previously reported that the expression of MAM-associated proteins is up-regulated in AD *postmortem* tissues and that primary neurons exposed to Aβ show an increased number of ER–mitochondria contacts as

*Correspondence to: Dr Maria ANKARCRONA
E-mail: maria.ankarcrona@ki.se

doi: 10.1111/jcmm.12863

detected by the proximity ligation assay [24]. Other studies show that the synthesis of cholesteryl esters and phospholipids is increased in fibroblasts derived from AD patients and in cells treated with apolipoprotein ε4-conditioned medium [14, 25].

Alzheimer's disease is a multifactorial neurodegenerative disease characterized by several neurological impairments. Pathological hallmarks include accumulation of extracellular amyloid plaques and intraneuronal fibrillary tangles [26–28]. The amyloid β-peptide (Aβ) is the main component of amyloid plaques. Aβ is generated *via* proteolytic processing of the amyloid-β precursor protein (APP) by two enzymes: β-site APP-cleaving enzyme 1 (BACE1) and the γ-secretase complex. The γ-secretase complex consists of four different proteins: Nicastrin (NCT), presenilin enhancer 2 (PEN-2), anterior pharynx-defective 1 (APH-1) and PS1 or PS2 [29–32]. In the amyloidogenic pathway, APP is first cleaved by BACE1 generating sAPPβ and C99. C99 is subsequently cleaved by γ-secretase to generate Aβ and APP intracellular domain (AICD) [29–32]. In the non-amyloidogenic pathway APP is first cleaved by α-secretase which generates sAPPα and C83. The C83 fragment is subsequently cleaved by γ-secretase generating a p3 fragment and AICD.

Several studies have shown enrichment of APP, PS1/PS2, Aβ as well as γ-secretase activity in lipid rafts and MAM [14, 33, 34]. Accordingly, we recently demonstrated that significant amounts of $A\beta_{40}$ and $A\beta_{42}$ are generated from MAM-enriched subcellular fractions of mouse brain [34]. Thus, a fraction of Aβ is generated in the vicinity of mitochondria, where it could exert a toxic effect.

Here, we have investigated the role of ER–mitochondria interplay in the regulation of Aβ production. Our data show that siRNA knockdown of Mfn2 results in increased contact between the two organelles leading to increased Ca^{2+} transfer from ER to mitochondria and decreased Aβ concentrations. Interestingly, γ-secretase complex maturation and activity is impaired in these conditions revealing a new mechanism by which cells regulate Aβ production.

Material and methods

Additional details are given in Data S1.

Cell viability and ATP levels

Cell viability was measured using the dye alamarBlue® (#DAL1025; Thermo Fisher Scientific, Waltham, MA, USA) and Mitochondrial ToxGlo™ (#G800; Promega , Madison, WI, USA). In the first assay, cells were incubated with 1× AlamarBlue® solution for 30 min. at 37°C, and part of the sample media was removed and fluorescence (λ_{ex} = 530–560 nm, λ_{em} = 580–610 nm) was measured. With Mitochondrial ToxGlo™ both cell viability and ATP levels were measured according to the manufacturer's protocol.

Transmission electron microscopy

Cells were pelleted and fixed in 2.5% (vol/vol) glutaraldehyde in 0.1 M phosphate buffer at room temperature, rinsed in 0.1 M phosphate buffer, post-fixed in 2% OsO_4 for 2 hrs, dehydrated in ethanol and acetone and finally embedded in LX-112 (Ladd, Burlington, VT, USA). Ultrathin sections were prepared using Leica Ultracut UCT (Leica, Wien, Austria) and contrasted with uranyl acetate followed by lead citrate. Specimens were examined in a Tecnai 12 BioTWIN transmission electron microscope (FEI Company, Eindhoven, The Netherlands) at 100 kV. Digital images were taken with a Veleta camera (Olympus Soft Imaging Solutions, GmbH, Münster, Germany) at a primary magnification of 20,500×. Pictures were then analysed using Image J software (National Institutes of Health, Bethesda, MD, USA).

Aequorin Ca^{2+} measurements

Aequorin measurements were performed as previously described [13] and are summarized in Data S1.

Determination of intra- and extracellular $A\beta_{40}$ and $A\beta_{42}$ concentrations

Twenty-four hours after the initiation of siRNA treatment cell medium was replaced by OptiMEM. After another 24 hrs, the OptiMEM was collected for quantification of extracellular Aβ levels. At the same time cells were lysed and intracellular Aβ levels measured. About 10 μg of protein from each sample (lysed cells or conditioned medium) was mixed with RIPA buffer and loaded in duplicates on the ELISA plate. The amounts of $A\beta_{40}$ and $A\beta_{42}$ were measured using the Human/rat $A\beta_{40}$ (#294-62501) or $A\beta_{42}$ (#290-62601) ELISA Kit Wako (Wako Chemicals, GmbH, Neuss, Germany) according to the manufacturer's instructions.

γ-secretase activity assay

All procedures were performed on ice or at 4°C. First, cells were harvested and spun down at 1500 × g, for 5 min. The supernatant was removed and pellet resuspended in buffer H [20 mM HEPES, 150 mM NaCl, 2 mM ethylenediaminetetraacetic acid (EDTA)]. Cells were then lysed by using G27 needles (Misawa) (130 strokes) and centrifuged at 1000 × g for 15 min. The pellet (nuclei fraction) was discarded while the supernatant (membrane fraction) was centrifuged at 100,000 × g for 1 hr. Pellet was then solubilized in buffer H containing 1% CHAPSO. Samples were shaken for 1 hr, and centrifuged again at 10,000 × g for 5 min. to remove insolubilized membranes. The supernatant was then diluted 1:2 with buffer H and 20 μg of protein incubated either with DMSO (control) or L-685,458 for 16 hrs at 37°C. Subsequently, sample buffer was added and Western blot analysis performed.

Neprilysin activity assay

Cells, grown in black 96-well plates with a clear bottom, were washed with 0.1 M MES (pH = 6.5) and incubated with substrate mix (0.1 M MES (pH = 6.5), 1× complete protease inhibitor (#786-331; G-Biosciences, Maryland Heights, MO, USA), 1 μM Z-Leu-Leu-Leu-H (aldehyde) (#3175; Peptide Institute, Osaka, Japan), 0.5 mM Suc-Ala-Ala-Phe-MCA (#S8758; Sigma-Aldrich, St. Louis, MO, USA) with or without 10 μM Thiorphan (#T6031; Sigma-Aldrich) for 1 hr at 37°C. The cells

Journal of Cellular and Molecular Medicine published by John Wiley & Sons Ltd and Foundation for Cellular and Molecular Medicine.

were then incubated with 15 μM Phosphoramidon (#4082; Peptide Institute) and 0.14 μl of LAPase (#L5006; Sigma-Aldrich) in a final volume of 100 μl. Reaction was stopped with 10 nM of EDTA and fluorescence was measured in a plate reader (λ_{Ex} = 355 nm, λ_{Em} = 460 nm). Differences between substrate mix with and without thiorphan represent neprilysin activity.

Statistical analysis

All data were analysed using IBM SPSS Statistics 22 software (IMB Corporation, New York, NY, USA). Data were evaluated for normal distribution using Kolmogorov–Sminorv test, checking the skewness of the distribution and Q–Q plot. Normally distributed data were compared by two-tailed independent-samples *t*-test. Not normally distributed data were compared by non-parametric, independent Mann–Whitney *U*-test. All values are expressed as mean ± S.E.M., *n* corresponds to number of independent experiments, $*P < 0.05$ and $**P < 0.001$ were considered to be significant.

Results

Cell viability and ATP levels are maintained during Mfn2 knockdown

HEK293 cells stably overexpressing APP Swedish mutation (HEK293 APPswe) were used as a model system. The Swedish double mutation (KM670/671NL), located close to the BACE1 cleavage site on APP, enhances generation of the γ-secretase substrate C99 and consequently Aβ [35–38]. Overexpression of APPswe in HEK293 cells was confirmed by Western blot (Fig. 1A). The expression of Mfn2 and mitochondrial marker translocase of the inner membrane subunit 23 (TIM23) was not affected by the APPswe overexpression (Fig. 1A). To modulate ER–mitochondria contacts, cells were treated with Mfn2 siRNA or negative control (NC) siRNA for 48 hrs (Fig. 1B). Downregulation of Mfn2 was accompanied by a slight increase in Mfn1 expression, while TIM23 expression was not affected (Fig. 1B).

The effect of Mfn2 knockdown on cell viability and energy production was investigated using the alamarBlue® and Mitochondrial ToxGlo™ assays. No differences in cell viability (reducing power and plasma membrane permeability) and ATP levels were detected between NC- and Mfn2 siRNA-treated cells (Fig. 1C and D). Analysis of cell morphology in a bright field microscope revealed that cells maintained their morphology during the treatment with Mfn2 siRNA (data not shown).

Knockdown of Mfn2 leads to extended ER–mitochondria contact length and increased Ca^{2+} transfer between the two organelles

The impact of Mfn2 knockdown on ER–mitochondria juxtaposition was analysed by transmission electron microscopy (TEM; Fig. 2A). In the analysis, ER–mitochondria contact was considered to be formed when the distance between the two membranes was ≤ 30 nm [2]. Mitofusin-2 knockdown increased the length of the ER stretches in contact with mitochondria, as compared to control (Fig. 2A and B). Accordingly, the percentage of the mitochondrial surface in contact with the ER increased in Mfn2 siRNA-treated cells, as compared to control (Fig. 2C). The number of ER–mitochondria contacts and mitochondria, and the mitochondria perimeter, were unaltered by Mfn2 siRNA (Fig. S1A and B). Mitochondrial morphology was affected, as shown by dilation of mitochondrial cristae in Mfn2 siRNA-treated cells (Fig. 2A).

To elucidate whether the increased physical coupling between the two organelles had a functional impact, we analysed the Ca^{2+} transfer from ER to mitochondria. An increased juxtaposition between the two organelles favours the shuttling of Ca^{2+}, while a decreased juxtaposition decreases the Ca^{2+} shuttling [39, 40]. To test the efficiency of Ca^{2+} transfer, HEK293 APPswe cells were cotransfected with cDNA encoding for the mitochondrial matrix-targeted Ca^{2+} probe, aequorin, and the Mfn2 (or NC) siRNA. After 48 hrs, cells were stimulated with ATP and carbachol (CCH) to induce an IP3-dependent ER Ca^{2+} release. A significant increase in mitochondrial Ca^{2+} peaks was observed upon Mfn2 siRNA knockdown, as compared to NC (Fig. 3A). These results show that mitochondrial Ca^{2+} uptake, upon ER Ca^{2+} release, can be modulated by the proximity of the two organelles. In addition, mitochondrial Ca^{2+} uptake may also depend on the amount of Ca^{2+} released from the ER facing mitochondria and on the levels of MCU. To investigate whether the two latter features contributed to the observed phenomenon, we first measured the cytosolic Ca^{2+} peaks obtained upon stimulation with ATP and CCH in cells expressing cytosolic aequorin (Fig. 3B). Secondly, we investigated mitochondrial Ca^{2+} uptake in permeabilized cells exposed to fixed amounts of Ca^{2+} (Fig. S2A and B). No significant differences were detected between NC- and Mfn2 siRNA-treated cells using these approaches (Fig. 3B and C, Fig. S2A and B). Furthermore, the protein levels of IP3R3 (mediating Ca^{2+} release from the ER) and VDAC1 and MCU (mediating mitochondrial Ca^{2+} uptake) were not affected by Mfn2 knockdown (Fig. 3D). Cytochrome c oxidase (COX IV) was used as a mitochondrial marker. These data are in accordance with our TEM results and show that Mfn2 knockdown in HEK293 APPswe cells results in an increased ER–mitochondria contact.

Knockdown of Mfn2 leads to decreased Aβ production *via* impairment of γ-secretase maturation and activity

Having established a cell model with increased ER–mitochondria contact, we next tested our hypothesis that the modulation of ER–mitochondria contact influences APP processing and Aβ production. Levels of intracellular and secreted Aβ were detected by a commercial ELISA. Interestingly, the levels of both intracellular and secreted $Aβ_{40}$ and $Aβ_{42}$ were decreased around 40% in cells treated with Mfn2 siRNA, as compared to NC siRNA (Fig. 4).

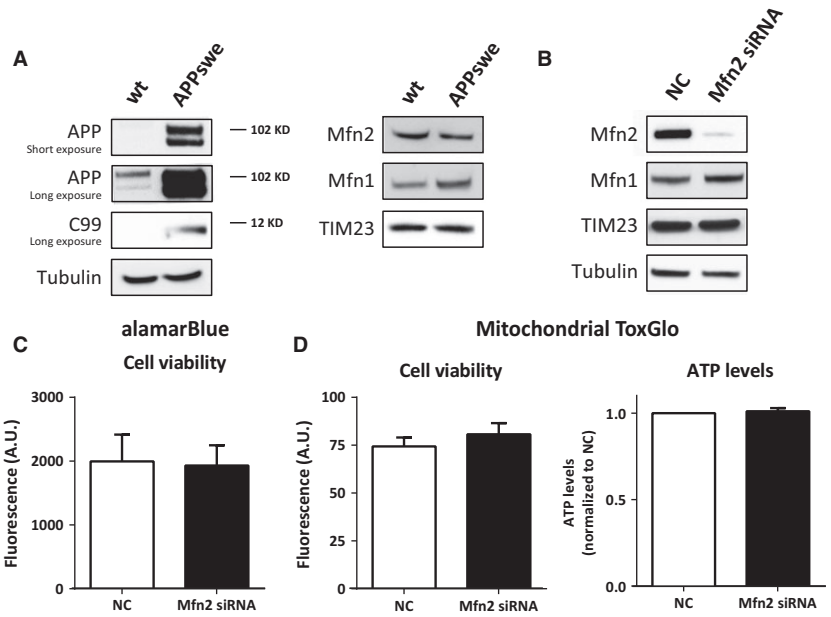

Fig. 1 Mfn2 siRNA knockdown in HEK293 cells stably overexpressing APPswe does not affect cell viability and ATP levels. (**A**) Whole cell homogenate of HEK293 WT and APPswe cells were subjected to SDS-PAGE and Western blot. Membranes were stained for indicated proteins. (**B**) Western blot of crude homogenate from HEK293 APPswe cells treated with NC or Mfn2 siRNA for 48 hrs. Membranes were stained for the indicated proteins. TIM23 was used as mitochondrial marker. (**C**) Cell viability (cytosolic reducing power) was measured using alamarBlue assay and presented in fluorescence arbitrary units (A.U.). (**D**) Cell viability measured as cell membrane permeability (fluorescence A.U.) and ATP levels (luminescence normalized to NC) were detected using Mitochondrial ToxGlo assay. Results are shown in mean ± S.E.M. of four independent experiments ($n = 4$) and duplicates for each condition. Mann–Whitney *U*-test was used for statistical analysis. NC: negative control; Mfn2 siRNA: siRNA for Mfn2 mRNA.

To elucidate whether the decrease in Aβ levels was as a result of impaired APP maturation, altered APP processing or increased Aβ degradation, we performed the following experiments. First, Western blot analysis revealed that the expression levels of total APP as well as of mature and immature APP were similar in Mfn2 siRNA- and NC siRNA-treated cells (Fig. 5A). Amyloid-β precursor protein is glycosylated in ER and Golgi and fully matured when reaching the plasma membrane [41]. The data show that this process is not affected by Mfn2 knockdown.

Second, we detected BACE1 and γ-secretase protein expression and measured γ-secretase activity. Western blot studies revealed that BACE1 levels were not changed in cells treated with Mfn2 siRNA. Interestingly, levels of PS1 and PS2 C- and N-terminal fragments (PS1/2-CTFs and PS1/2-NTFs) were significantly reduced (Fig. 5A) after Mfn2 knockdown. Moreover, levels of PEN-2 and immature NCT increased, while APH-1 levels were unaltered in Mfn2 siRNA-treated cells (Fig. 5A). γ-Secretase activity was measured in an assay detecting AICD formation from membrane fractions incubated overnight in the absence or presence of the γ-secretase inhibitor L-685,458. Decreased AICD production was detected in cells treated with Mfn2 siRNA as compared to NC siRNA (Fig. 5B, Fig. S3C). Levels of C83 and C99 were unaltered (Fig. 5B, Fig. S3A and B). In this assay, membrane fractions isolated from siRNA-treated cells were incubated in a 1% CHAPSO buffer for 16 hrs. The amounts of AICD, formed from the γ-secretase substrates C83/C99, were subsequently detected by Western blot. Our results show that sufficient amounts of C83/C99 were present in the membrane fraction, and thus decreased AICD levels reflect lower γ-secretase activity in Mfn2 siRNA-treated cells as compared to NC siRNA-treated cells. Altogether these data show that increased ER–mitochondria contact negatively affects γ-secretase complex maturation and activity.

Finally, we investigated both activity and protein levels of neprilysin. Neprilysin is a membrane-bound zinc-dependent metalloprotease that degrades different peptides, including Aβ. Neprilysin has been shown to be one of the major Aβ-degrading enzymes [42]. Neprilysin activity and protein expression were similar in Mfn2 siRNA-treated cells as compared to NC siRNA-treated cells (Fig. 5C). These data show that decreased Aβ concentrations in Mfn2 siRNA-treated cells were not because of the increased peptide degradation by neprilysin.

Discussion

In the recent years altered functions of MAM and ER–mitochondria communication have been described in disorders such as AD, cardiovascular disease and obesity [14, 24, 43, 44]. In this study we show that Mfn2 knockdown increases ER–mitochondria juxtaposition, decreases levels of intracellular and secreted Aβ and impairs γ-secretase activity.

Journal of Cellular and Molecular Medicine published by John Wiley & Sons Ltd and Foundation for Cellular and Molecular Medicine.

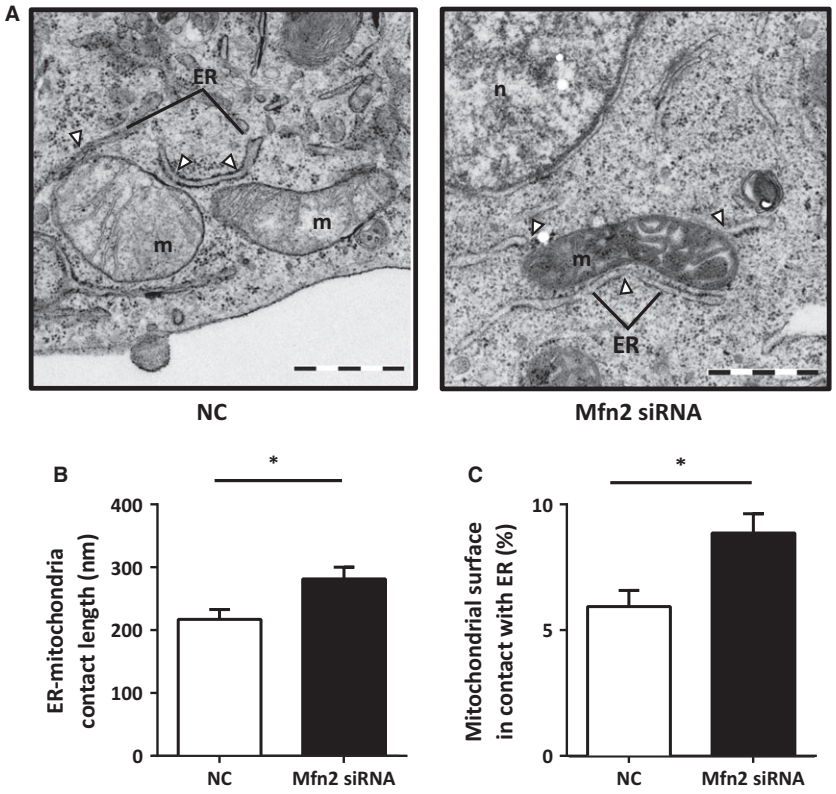

Fig. 2 Mfn2 knockdown increases ER–mitochondria contacts. (**A**) Representative electron micrographs of HEK293 APPswe treated either with NC (left panel) or Mfn2 siRNA (right panel). Pictures were taken at a magnification of 20,500×. (**B**) Quantification of contact length in NC and Mfn2 si RNA-treated cells. (**C**) Ratio between total length of contacts and total mitochondrial perimeter per cell. Number of cells analysed varied between $19 \leq n \leq 25$. Results are shown as mean ± S.E.M. of three independent experiments. Independent *t*-test was used for statistical analysis. $*P < 0.05$. NC: negative control; Mfn2 siRNA: siRNA for Mfn2 mRNA. Scale bars correspond to 1 μm.

The pathway for Aβ generation is well-established, however the intracellular regulation of this process is not fully understood [29–32]. Several proteins have been shown to modulate γ-secretase activity and thus Aβ production (*e.g.* VDAC1, γ-secretase-activating protein, reticulon protein family). These proteins present different functions and subcellular localizations within the cell [45–48]. Still, the exact mechanisms of how these proteins modulate γ-secretase activity remain to be elucidated. Here, we have tested an alternative hypothesis proposing that modulation of ER–mitochondria contacts affects Aβ generation.

Mfn2 has been described to have an essential role in the tethering of ER and mitochondria [6–9]. As a result of its specific location and function at ER–mitochondria contacts, the ablation or reduction of this protein has been used for the modulation of ER–mitochondria contacts [6–9, 15]. However, the role of Mfn2 as a tethering protein between ER and mitochondria has recently been questioned by us and others [7–9]. In the present study, Ca^{2+} measurements and TEM-analysis show that the knockdown of Mfn2 results in increased coupling between ER and mitochondria. This is in accordance with recent publications proposing that Mfn2 works as an ER–mitochondria tetheering antagonist [7–9].

Mfn2 siRNA treatment also resulted in dilated mitochondrial cristae, supporting the importance of Mfn2 in mitochondrial morphology. Mitofusin-1 and -2 seem to have partially redundant physiological functions, where Mfn1 can compensate for Mfn2 reduction and *vice versa* [49, 50]. Accordingly, our data show that Mfn1 protein levels were slightly increased in cells treated with Mfn2 siRNA. Thus, Mfn1 could compensate for Mfn2 knockdown in terms of energy production and cell viability but not in terms of mitochondrial morphology.

In our model, the knockdown of Mfn2 siRNA and the increase in ER–mitochondria Ca^{2+} transfer did not cause mitochondrial failure and cell death (at least not within the treatment period). Ca^{2+} is crucial for cell homoeostasis. Upon certain stimuli the levels of Ca^{2+} in the cytosol can rise. Mitochondria have the ability to rapidly buffer such increased cytosolic Ca^{2+} by accumulating Ca^{2+} in the matrix. This buffering tunes overall Ca^{2+} signalling within the cell [51]. Moreover, changes in mitochondrial Ca^{2+} levels can have an impact in the metabolic regulation of Ca^{2+}-activated matrix dehydrogenases, thus modulating ATP production [51–55]. In fact, small Ca^{2+} changes within mitochondria (0.1–10 μM) can lead to major changes inside the cell [51–55]. Disruption of Ca^{2+} homoeostasis as a result of the long or intense treatments/stimuli can lead to cell death (*e.g.* overload of mitochondrial Ca^{2+} triggers apoptosis). Several studies have shown that PS mutations lead to changes in Ca^{2+} homoeostasis by increasing cytosolic Ca^{2+} [56–58]. It has also been shown that PS1 and PS2 have a γ-secretase-independent role in the regulation of calcium homoeostasis and tethering between ER and mitochondria [13, 56]. Moreover, it has been shown that increased cytosolic Ca^{2+} leads to decreased APP levels and subsequently decreased Aβ production [59]. However, in our study, Mfn2 knockdown did not result in an alteration in the bulk cytosolic Ca^{2+} concentration, neither at rest nor upon cell stimulation. Instead, the specific increase in Ca^{2+} transfer from ER to mitochondria (further

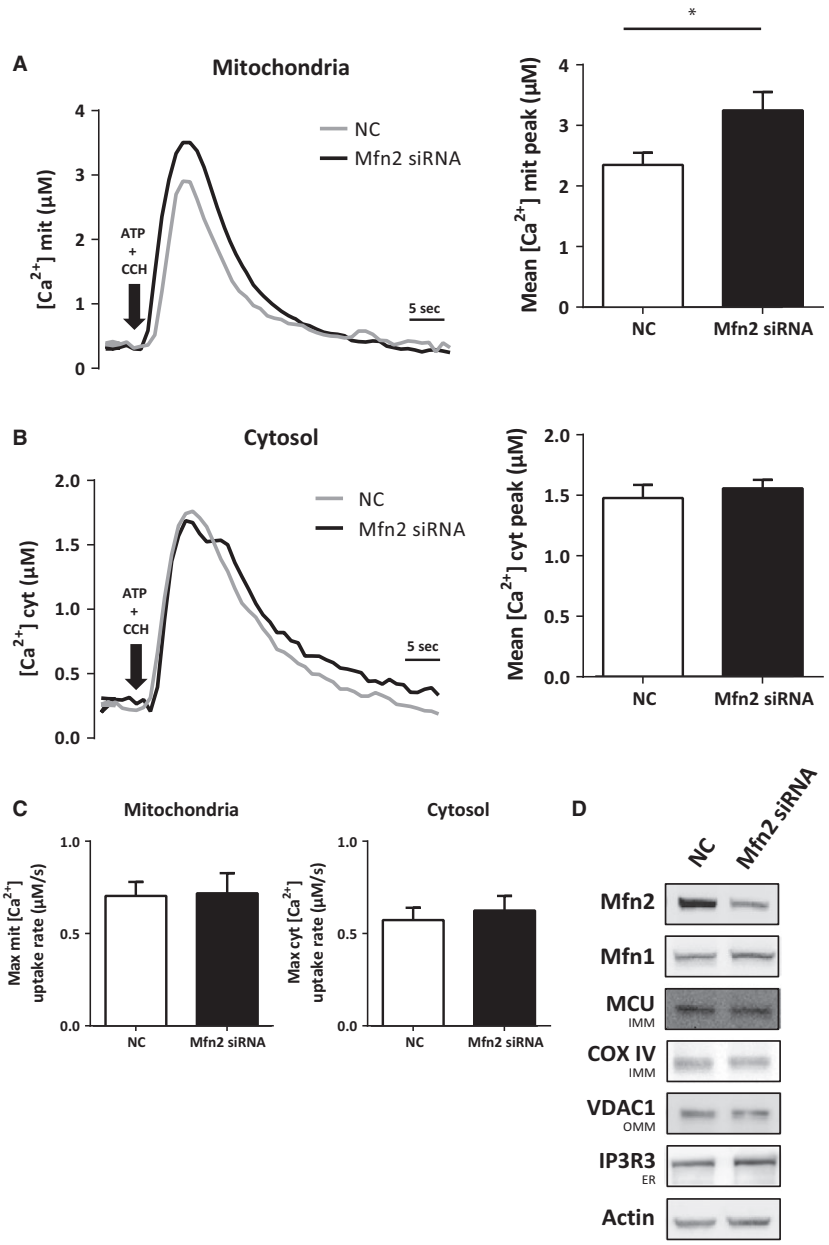

Fig. 3 Mfn2 knockdown increases Ca^{2+} transfer between ER and mitochondria. (**A**) Mitochondrial Ca^{2+} peak upon stimulation of ER Ca^{2+} release with ATP and carbachol (CCH) or (**B**) cytosolic Ca^{2+} peak in NC and Mfn2 siRNA-treated cells and (**C**) respective rise rates. Sample size varied between $8 \leq n \leq 10$ (independent experiments), with triplicates for each condition. Results are shown in mean ± S.E.M. Independent *t*-test was used for statistical analysis. $*P < 0.05$. (**D**) Western blot of whole cell homogenates from cells treated either with NC or Mfn2 siRNA. Membranes were stained for indicated proteins. COX IV was used as a mitochondria marker NC: negative control; Mfn2 siRNA: siRNA for Mfn2 mRNA.

demonstrating a straitened coupling between the two organelles) suggests that the observed decreased γ-secretase activity and Aβ levels were not caused by alterations in cytosolic Ca^{2+}. However, further investigations need to be done to understand the mechanism by which altered ER–mitochondria contact and Ca^{2+} transfer affect γ-secretase maturation, assembly and activity.

Here, quantitative measurements of intra- and extracellular $A\beta_{40}$ and $A\beta_{42}$ in cells treated with Mfn2 siRNA showed that increased ER–mitochondria contact decreased Aβ levels. Possible mechanisms behind this decrease in Aβ generation include: (*i*) decreased levels or impaired maturation of APP, (*ii*) decreased expression of BACE1 and/or γ-secretase proteins and/or activities, (*iii*) increased degradation of Aβ. Firstly, our data show that APP protein levels were unaltered and that mature APP was available for BACE1 and γ-secretase cleavage in cells treated with Mfn2 siRNA. Secondly, BACE1 protein levels were unaltered and degradation of Aβ was not enhanced as measured by a neprilysin activity assay. Thirdly, alterations in the expression and maturation of γ-secretase complex components were identified along with decreased γ-secretase activity. The γ-secretase complex assembles and matures in the secretory pathway. Nicastrin and APH-1 first form a scaffolding complex to which PS1 (or PS2) binds. Presenilin enhancer 2 stabilizes this complex and activates endoproteolysis of

Journal of Cellular and Molecular Medicine published by John Wiley & Sons Ltd and Foundation for Cellular and Molecular Medicine.

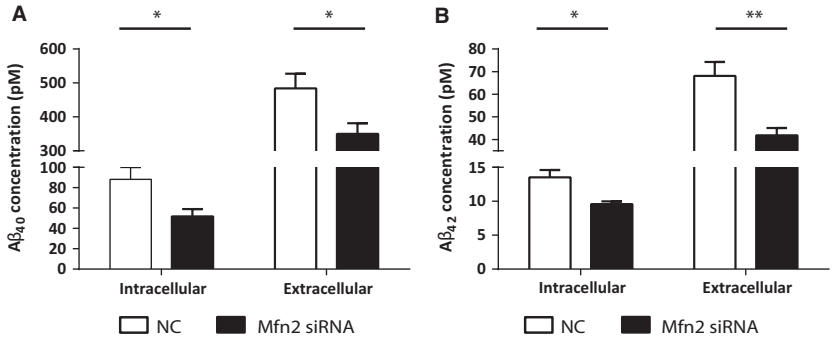

Fig. 4 Mfn2 down-regulation decreases intracellular and secreted levels of Aβ. Intra- and extracellular levels of (**A**) $A\beta_{40}$ and (**B**) $A\beta_{42}$ were assessed by ELISA. $4 \leq n \leq 9$ (independent experiments), with duplicates for each condition. Results are shown as mean ± S.E.M. Mann–Whitney *U*-test was used for statistical analysis. $*P < 0.05$, $**P < 0.001$. NC: negative control; Mfn2 siRNA: siRNA for Mfn2 mRNA.

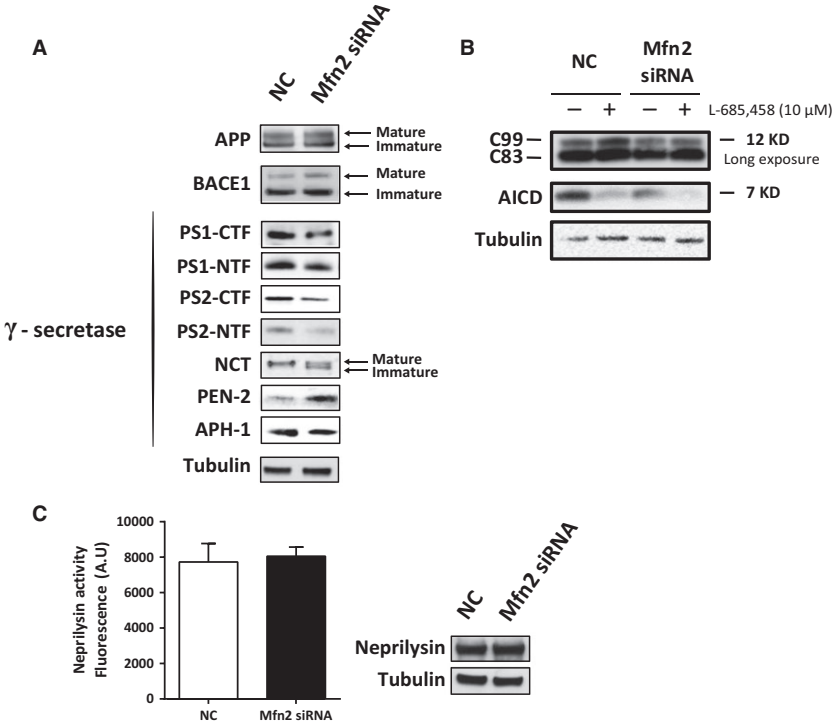

Fig. 5 Mfn2 knockdown leads to impaired γ-secretase activity and maturation. (**A**) Protein expression of APP, BACE1 and γ-secretase components was assessed by Western blot analysis of cell homogenates from NC and Mfn2 siRNA-treated cells. (**B**) γ-secretase activity assay using a membrane fraction from cells treated with NC or Mfn2 siRNA in the presence or absence of γ-secretase inhibitor L-685,458. APP fragments (C99, C83, AICD) were detected using the Y188 antibody. (**C**) Intact cells were treated with NC or Mfn2 siRNA and incubated with specific neprilysin peptide. Neprilysin activity was investigated by measuring the fluorescence of cleaved peptide (arbitrary units). Western blots of cell homogenates were performed. $n = 4$ (independent experiments), with duplicates or triplicates for each condition. Results are shown in mean ± S.E.M. Mann–Whitney *U*-test was used for statistical analysis NC: negative control; Mfn2 siRNA: siRNA for Mfn2 mRNA.

PS1 (or PS2) [29–32]. Moreover, it has been shown that APP and active γ-secretase complexes are enriched in lipid rafts [24, 33, 60, 61] of the plasma membrane, endosomes, autophagosomes, synaptosomes and MAM [14–16]. Lipid rafts are thus important sites for Aβ production [34, 61]. Here we detected both mature and immature NCT in Mfn2 siRNA-treated cells, while cells treated with control siRNA only expressed mature NCT. APH-1 levels were not affected by Mfn2 knockdown. The presence of immature NCT suggests that less scaffolding complexes are available for binding of PS1 (or PS2) and PEN2 under these conditions. In addition, we show that the protein levels of PS1 and PS2 (NTFs and CTFs) were decreased when Mfn2 is knocked down. γ-Secretase complexes containing endoproteolysed PS1 are mainly responsible for the generation of Aβ, while γ-secretase complexes containing PS2 are less active in cleaving C99 [29–32]. PEN-2 protein levels were increased in Mfn2 siRNA-treated cells suggesting that PEN2 was not a limiting factor for endoproteolysis of PS. Importantly, decreased γ-secretase activity, as measured by AICD formation, was detected. Thus, the presence of immature NCT and low levels of PS1-NTFs and CTFs are likely the cause of low γ-secretase activity in cells treated with Mfn2 siRNA. These results are in accordance with previous studies showing that mouse embryonic fibroblast cells lacking Mfn2 (MEF Mfn2-KO) present a decreased activity of γ-secretase [14].

To elucidate the exact relation between ER–mitochondria contacts and γ-secretase activity more experiments need to be done. At present we can only speculate about the mechanisms behind the impairment of γ-secretase complex assembly and activity. Changes in phospholipid and cholesterol metabolism and calcium homoeostasis

have been linked to AD [14, 16, 62, 63]. As previously mentioned, APP and active γ-secretase complexes are enriched in lipid rafts [24, 33, 60, 61]. Mitochondria-associated ER membranes are crucial for biosynthesis of different phospholipids and cholesterol. Therefore, modulation of ER–mitochondria contact may alter MAM function and phospholipid/
cholesterol synthesis resulting in altered lipid raft composition and γ-secretase activity [14, 32, 33, 63]. Furthermore, if we consider the importance of the phospholipids produced at MAM for vesicle formation, modulation of ER–mitochondria contacts could lead to altered transport/localization of γ-secretase complexes inside the cell.

In summary, we show that γ-secretase complex maturation and activity is affected by increased ER–mitochondria contact leading to decreased Aβ levels. More experiments are required to determine if ER–mitochondria contacts can be modulated to specifically target cleavage of APP without affecting other γ-secretase substrates. Even though ablation of Mfn2 is not a realistic treatment strategy, because of the importance of this protein for long-term mitochondrial stability, our data show that acute modulation of ER–mitochondria contact affects γ-secretase assembly and function. This finding opens up for new strategies to modulate γ-secretase activity, apart from γ-secretase inhibitors and modulators. Altogether, the present data reinforce other studies suggesting that modulation of MAM functions and ER–mitochondria communication may hold potential as novel drug targets for future AD therapy.

Acknowledgements

The authors would like to thank: Dr Kjell Hultenby (Dept Laboratory Medicine; Karolinska Institutet, Huddinge, Sweden) for excellent help with transmission electron microscopy, Dr Per Nilsson (Laboratory for Proteolytic Neuroscience, RIKEN Brain Science Institute, Wako Saitama, Japan and Dept NVS, Karolinska Institutet, Huddinge, Sweden) for the neprilysin assay protocol, Dr Susanne Frykman (Dept NVS, Karolinska Institutet, Huddinge, Sweden) for help with establishing the siRNA transfection protocol and Dr Johan Lundkvist (Alzecure Foundation, Stockholm, Sweden) for the kind gift of HEK293-APPswe cells. These studies were supported grants from: The Swedish Alzheimer Foundation, Gamla Tjänarinnor Foundation, Stohnes Stiftelse, Dementia Foundation, the Foundation for Geriatric Diseases at Karolinska Institutet and the Swedish Research Council (K2012-61X-22097-01-3). Karolinska Institutet Doctoral Grant and Sven and Lilly Lawskis Fund for Natural Science Research to NSL. The German Research Foundation to BS. A donation from Peter Thelin's family to MA. Fondazione Cassa di Risparmio di Padova e Rovigo (CARIPARO Foundation; Progetti d'eccellenza 2011/2012) to RF and PP.

Conflict of interest

The authors confirm that there are no conflicts of interest.

Author contribution

NSL, BS, CMP, BW and RF performed the research; NSL, BS, RF, PP and MA designed the research study; NSL, BS, CMP, RF, PP and MA analysed the data; NSL, RF, PP and MA wrote the paper.

Supporting information

Additional Supporting Information may be found online in the supporting information tab for this article:

Figure S1 Mfn2 knockdown does neither change mitochondria or contact numbers nor mitochondrial perimeter. (**A**) Quantification of the number of mitochondria and contacts in HEK293 APPswe treated either with NC or Mfn2 siRNA (**B**) quantification of mitochondrial perimeter. Quantifications were performed with Image J. Number of cells analysed varied between $19 \leq n \leq 25$. Results are shown in mean ± S.E.M. of three independent experiments. Independent *t*-test was used for statistical analysis. NC: negative control; Mfn2 siRNA: siRNA for Mfn2 mRNA.

Figure S2 Mfn2 down-regulation neither changes the Ca^{2+} uptake by mitochondria in permeabilized cells nor the rate of Ca^{2+} uptake. (**A**) Mitochondrial Ca^{2+} uptake in permeabilized cells exposed to specific Ca^{2+} concentrations, measured by a mitochondrial aequorin as Ca^{2+} probe. (**B**) Respective Ca^{2+} uptake rate. Sample size varied between $3 \leq n \leq 4$ (independent experiments), with triplicates for each condition. Results are shown in mean ± S.E.M. Mann–Whitney *U*-test was used for statistical analysis. NC: negative control; Mfn2 siRNA: siRNA for Mfn2 mRNA.

Figure S3 Mfn2 knockdown leads to changes in AICD levels, while C99 or C83 levels remain unaltered. Quantification of (**A**) C83, (**B**) C99 and (**C**) AICD bands from Figure 5. Results are shown in mean ± S.E.M. $4 \leq n \leq 6$. Mann–Whitney *U*-test was used for statistical analysis. NC: negative control; Mfn2 siRNA: siRNA for Mfn2 mRNA. Membrane fractions were incubated in the presence (+) or absence (-) of 10 μM L-685,458 (γ-secretase inhibitor).

Data S1 Material and methods.

References

1. **Raturi A, Simmen T.** Where the endoplasmic reticulum and the mitochondrion tie the knot: the mitochondria-associated membrane (MAM). *Biochim Biophys Acta - Mol Cell Res.* 2013; 1833: 213–24.
2. **Csordás G, Renken C, Várnai P, *et al.*** Structural and functional features and significance of the physical linkage between ER and mitochondria. *J Cell Biol.* 2006; 174: 915–21.
3. **de Brito OM, Scorrano L.** An intimate liaison: spatial organization of the endoplasmic reticulum-mitochondria relationship. *EMBO J.* 2010; 29: 2715–23.

Journal of Cellular and Molecular Medicine published by John Wiley & Sons Ltd and Foundation for Cellular and Molecular Medicine.

4. **Merkwirth C, Langer T.** Mitofusin 2 builds a bridge between ER and mitochondria. *Cell*. 2008; 135: 1165–7.
5. **Simmen T, Aslan JE, Blagoveshchenskaya AD, *et al.*** PACS-2 controls endoplasmic reticulum-mitochondria communication and Bid-mediated apoptosis. *EMBO J*. 2005; 24: 717–29.
6. **de Brito OM, Scorrano L.** Mitofusin 2 tethers endoplasmic reticulum to mitochondria. *Nature*. 2008; 456: 605–10.
7. **Cosson P, Marchetti A, Ravazzola M, *et al.*** Mitofusin-2 independent juxtaposition of endoplasmic reticulum and mitochondria: an ultrastructural study. *PLoS ONE*. 2012; 7: 1–5.
8. **Filadi R, Greotti E, Turacchio G, *et al.*** Mitofusin 2 ablation increases endoplasmic reticulum–mitochondria coupling. *Proc Natl Acad Sci USA*. 2015; 112: E2174–81.
9. **Wang PTC, Garcin PO, Fu M, *et al.*** Distinct mechanisms controlling rough and smooth endoplasmic reticulum-mitochondria contacts. *J Cell Sci*. 2015; 128: 2759–65.
10. **Giorgi C, Missiroli S, Patergnani S, *et al.*** Mitochondria-associated membranes: composition, molecular mechanisms, and physiopathological implications. *Antioxid Redox Signal*. 2015; 22: 995–1019.
11. **Szabadkai G, Bianchi K, Várnai P, *et al.*** Chaperone-mediated coupling of endoplasmic reticulum and mitochondrial Ca^{2+} channels. *J Cell Biol*. 2006; 175: 901–11.
12. **Naon D, Scorrano L.** At the right distance: ER-mitochondria juxtaposition in cell life and death. *Biochim Biophys Acta - Mol Cell Res*. 2014; 1843: 2184–94.
13. **Zampese E, Fasolato C, Kipanyula MJ, *et al.*** Presenilin 2 modulates endoplasmic reticulum (ER)-mitochondria interactions and Ca^{2+} cross-talk. *Proc Natl Acad Sci USA*. 2011; 108: 2777–82.
14. **Area-Gomez E, Del Carmen Lara Castillo M, Tambini MD, *et al.*** Upregulated function of mitochondria-associated ER membranes in Alzheimer disease. *EMBO J*. 2012; 31: 4106–23.
15. **Hamasaki M, Furuta N, Matsuda A, *et al.*** Autophagosomes form at ER-mitochondria contact sites. *Nature*. 2013; 495: 389–93.
16. **Hayashi T, Rizzuto R, Hajnoczky G, *et al.*** MAM: more than just a housekeeper. *Trends Cell Biol*. 2009; 19: 81–8.
17. **Poston CN, Krishnan SC, Bazemore-Walker CR.** In-depth proteomic analysis of mammalian mitochondria-associated membranes (MAM). *J Proteomics*. 2013; 79: 219–30.
18. **Stefani M, Liguri G.** Cholesterol in Alzheimer's disease: unresolved questions. *Curr Alzheimer Res*. 2009; 6: 15–29.
19. **Pettegrew JW, Panchalingam K, Hamilton RL, *et al.*** Brain membrane phospholipid alterations in Alzheimer's disease. *Neurochem Res*. 2001; 26: 771–82.
20. **Gillardon F, Rist W, Kussmaul L, *et al.*** Proteomic and functional alterations in brain mitochondria from Tg2576 mice occur before amyloid plaque deposition. *Proteomics*. 2007; 7: 605–16.
21. **Fraser T, Tayler H, Love S.** Fatty acid composition of frontal, temporal and parietal neocortex in the normal human brain and in Alzheimer's disease. *Neurochem Res*. 2010; 35: 503–13.
22. **Bezprozvanny I, Mattson MMP.** Neuronal calcium mishandling and the pathogenesis of Alzheimer's disease. *Trends Neurosci*. 2008; 31: 454–63.
23. **Wang X, Su B, Zheng L, *et al.*** The role of abnormal mitochondrial dynamics in the pathogenesis of Alzheimer's disease. *J Neurochem*. 2009; 109: 153–9.
24. **Hedskog L, Moreira C, Filadi R, *et al.*** Modulation of the endoplasmic reticulum – mitochondria interface in Alzheimer's disease and related models. *Proc Natl Acad Sci USA*. 2013; 110: 7916–21.
25. **Tambini MD, Pera M, Kanter E, *et al.*** ApoE 4 upregulates the activity of mitochondria-associated ER membranes. *EMBO Rep*. 2016; 17: 27–36.
26. **Association A.** 2012 Alzheimer's disease facts and figures. *Alzheimers Dement*. 2012; 8: 131–68.
27. **Kumar A, Singh A, Ekavali .** A review on Alzheimer's disease pathophysiology and its management: an update. *Pharmacol Reports*. 2015; 67: 195–203.
28. **Ramirez-Bermudez J.** Alzheimer's disease: critical notes on the history of a medical concept. *Arch Med Res*. 2012; 43: 595–9.
29. **De Strooper B.** Aph-1, Pen-2, and Nicastrin with Presenilin generate an active Gamma-Secretase complex. *Neuron*. 2003; 38: 9–12.
30. **St George-Hyslop P, Fraser PE.** Assembly of the presenilin γ-/ε-secretase complex. *J Neurochem*. 2012; 120 (Suppl.): 84–8.
31. **Gertsik N, Chiu D, Li Y-M.** Complex regulation of γ-secretase: from obligatory to modulatory subunits. *Front Aging Neurosci*. 2015; 6: 1–10.
32. **Smolarkiewicz M, Skrzypczak T.** The very many faces of presenilins and the γ -secretase complex. *Protoplasma*. 2013; 250: 997–1011.
33. **Urano Y, Hayashi I, Isoo N, *et al.*** Association of active gamma-secretase complex with lipid rafts. *J Lipid Res*. 2005; 46: 904–12.
34. **Schreiner B, Hedskog L, Wiehager B, *et al.*** Amyloid-β peptides are generated in mitochondria-associated endoplasmic reticulum membranes. *J Alzheimers Dis*. 2015; 43: 369–74.
35. **Mullan M, Crawford F, Axelman K, *et al.*** A pathogenic mutation for probable Alzheimer's disease in the APP gene at the N–terminus of β–amyloid. *Nature*. 1992; 1: 345–7.
36. **Johnston JA, Cowburn RF, Norgren S, *et al.*** Increased beta-amyloid release and levels of amyloid precursor protein (APP) in fibroblast cell lines from family members with the Swedish Alzheimer's disease APP670/671 mutation. *Neurosciences*. 1994; 354: 274–8.
37. **Citron M, Oltersdorf T, Haass C, *et al.*** Mutation of the beta-amyloid precursor protein in familial Alzheimer's disease increases beta-protein production. *Nature*. 1992; 360: 672–4.
38. **Citron M, Vigo-Pelfrey C, Teplow DB, *et al.*** Excessive production of amyloid beta-protein by peripheral cells of symptomatic and presymptomatic patients carrying the Swedish familial Alzheimer disease mutation. *Proc Natl Acad Sci USA*. 1994; 91: 11993–7.
39. **Csordás G, Várnai P, Golenár T, *et al.*** Imaging interorganelle contacts and local calcium dynamics at the ER-mitochondrial interface. *Mol Cell*. 2010; 39: 121–32.
40. **Giacomello M, Drago I, Bortolozzi M, *et al.*** Ca^{2+} hot spots on the mitochondrial surface are generated by Ca^{2+} mobilization from stores, but not by activation of store-operated Ca^{2+} channels. *Mol Cell*. 2010; 38: 280–90.
41. **Schedin-Weiss S, Winblad B, Tjernberg LO.** The role of protein glycosylation in Alzheimer disease. *FEBS J*. 2014; 281: 46–62.
42. **Grimm MOW, Mett J, Christoph P, *et al.*** Neprilysin and Aβ clearance: impact of the APP intracellular domain in NEP regulation and implications in Alzheimer's disease. *Front Aging Neurosci*. 2013; 5: 1–27.
43. **Paillard M, Tubbs E, Thiebaut P-A, *et al.*** Depressing mitochondria-reticulum interactions protects cardiomyocytes from lethal hypoxia-reoxygenation injury. *Circulation*. 2013; 128: 1555–65.
44. **Arruda AP, Pers BM, Parlakgül G, *et al.*** Chronic enrichment of hepatic endoplasmic reticulum–mitochondria contact leads to mitochondrial dysfunction in obesity. *Nat Med*. 2014; 20: 1927–35.
45. **Teranishi Y, Inoue M, Yamamoto NG, *et al.*** Proton myo-inositol cotransporter is a novel γ-secretase associated protein that regulates Aβ production without affecting Notch cleavage. *FEBS J*. 2015; 282: 3438–51.

46. **Frykman S, Teranishi Y, Hur J-Y, *et al.*** Identification of two novel synaptic γ-secretase associated proteins that affect amyloid β-peptide levels without altering Notch processing. *Neurochem Int*. 2012; 61: 108–18.
47. **Hur J-Y, Teranishi Y, Kihara T, *et al.*** Identification of novel γ-secretase-associated proteins in detergent-resistant membranes from brain. *J Biol Chem*. 2012; 287: 11991–2005.
48. **Tang BL, Liou YC.** Novel modulators of amyloid-beta precursor protein processing. *J Neurochem*. 2007; 100: 314–23.
49. **Cipolat S, Martins de Brito O, Dal Zilio B, *et al.*** OPA1 requires mitofusin 1 to promote mitochondrial fusion. *Proc Natl Acad Sci USA*. 2004; 101: 15927–32.
50. **Chen H, Detmer SA, Ewald AJ, *et al.*** Mitofusins Mfn1 and Mfn2 coordinately regulate mitochondrial fusion and are essential for embryonic development. *J Cell Biol*. 2003; 160: 189–200.
51. **Rizzuto R, De Stefani D, Raffaello A, *et al.*** Mitochondria as sensors and regulators of calcium signalling. *Nat Rev Mol Cell Biol*. 2012; 13: 566–78.
52. **Babcock DF, Herrington J, Goodwin PC, *et al.*** Mitochondrial Participation in the Intracellular Ca^{2+} Network. *J Cell Biol*. 1997; 136: 833–44.
53. **Denton M, Martin BR.** Stimulation by calcium ions of pyruvate dehydrogenase phosphate phosphatase. *J Biochem*. 1972; 128: 161–3.
54. **Denton BRM, Richards DA, Chin JG.** Calcium ions and the regulation of NAD + -linked isocitrate dehydrogenase from the mitochondria of rat heart and other tissues. *J Biochem*. 1978; 176: 899–906.
55. **Traaseth N, Elfering S, Solien J, *et al.*** Role of calcium signaling in the activation of mitochondrial nitric oxide synthase and citric acid cycle. *Biochim Biophys Acta*. 2004; 1658: 64–71.
56. **Lee JH, McBrayer MK, Wolfe DM, *et al.*** Presenilin 1 maintains lysosomal Ca^{2+} homeostasis *via* TRPML1 by regulating vAT-Pase-mediated lysosome acidification. *Cell Rep*. 2015; 12: 1430–44.
57. **Tu H, Nelson O, Bezprozvanny A, *et al.*** Presenilins form ER Ca^{2+} leak channels, a function disrupted by familial Alzheimer's disease-linked mutations. *Cell*. 2006; 126: 981–93.
58. **Bello BC, Izergina N, Caussinus E, *et al.*** Amplification of neural stem cell proliferation by intermediate progenitor cells in Drosophila brain development. *Neural Dev*. 2008; 3: 5.
59. **Jung ES, Hong H, Kim C, *et al.*** Acute ER stress regulates amyloid precursor protein processing through ubiquitin-dependent degradation. *Sci Rep*. 2015; 5: 8805.
60. **Area-Gomez E, de Groof AJC, Boldogh I, *et al.*** Presenilins are enriched in endoplasmic reticulum membranes associated with mitochondria. *Am J Pathol*. 2009; 175: 1810–6.
61. **Araki W, Tamaoka A.** Amyloid beta-protein and lipid rafts: focused on biogenesis and catabolism. *Front Biosci*. 2015; 20: 314–24.
62. **Smith IF, Green KN, LaFerla FM.** Calcium dysregulation in Alzheimer's disease: recent advances gained from genetically modified animals. *Cell Calcium*. 2005; 38: 427–37.
63. **Vance JE.** MAM (mitochondria-associated membranes) in mammalian cells: lipids and beyond. *Biochim Biophys Acta - Mol Cell Biol Lipids*. 2014; 1841: 595–609.

Journal of Cellular and Molecular Medicine published by John Wiley & Sons Ltd and Foundation for Cellular and Molecular Medicine.